



25 March 1994

**CHEMICAL  
PHYSICS  
LETTERS**

Chemical Physics Letters 220 (1994) 35–39

## Dynamics of the sol–gel transition in organic–inorganic nanocomposites

P. Judeinstein<sup>1</sup>, P.W. Oliveira, H. Krug, H. Schmidt

*Institut für Neue Materialien, Universität des Saarlandes, Geb. 43, W-6600 Saarbrücken, Germany*

Received 16 December 1993

### Abstract

Two different techniques have been used to follow the gelation of photochromic organic–inorganic nanocomposites. The variations of molecular and macromolecular motions in these complex systems have been analyzed. Photo-correlation spectroscopy probes the formation of the gel network. Forced Rayleigh scattering experiences the microstructure of the mixtures via the measurement of the translational diffusion coefficient of entrapped photoreactive targets. In the different mixtures, a drop of the network mobility could be observed around the sol to gel conversion, while the entrapped molecules do not experience the macroscopic transition.

### 1. Introduction

For the last few years, a great amount of scientific and technological work has been devoted to hybrid organic–inorganic materials [1,2]. This class of totally innovative materials should synergize properties of both components. The organic phase could be entrapped inside a well-suited oxide network or linked to metal atoms, and could be used to develop the material structure or to tune the properties, leading to many applications [3].

These sophisticated materials are complex edifices, and must be described as multifold frameworks in regard to the different topological scales. Then, multispectroscopic analysis has to be performed to probe their structure as far as possible.

Nevertheless, the optimization of their properties is also strongly related to the dynamical behavior in-

side such blends. The knowledge of stiffnesses and motion processes of molecular and macromolecular units from the reactant's mixing instant to the material itself is essential to control the film quality and finally physical properties. Some attempts to obtain such data have already been described for some metal oxide or hybrid gels. The real problem is to get data about their diphasic aspect: a 'solid' network entrapping a 'liquid' phase. Two sets of experiments have been proposed to explore these mixtures. Firstly, the dynamics of the molecules forming the network has been probed during the conversion with viscosity, rheology, NMR or dynamic light scattering [4]. On the other side, the properties of the gels have been described through the behavior of entrapped probes with typical features: electrochemistry active [5], rigidochromic or polarization fluorescence [4,6], non-linear optics [7].

Recently, we have described two families of transparent nanocomposites presenting electrochemical and photochromic properties [8,9]. They are obtained by entrappment of heteropolymetalates

<sup>1</sup> Present address: Laboratoire de Chimie Structurale Organique (URA CNRS 1384), Université Paris-Sud, Bâtiment 410, 91405 Orsay, France.

(POM) inside organic–inorganic structures. Their moderate electrochemical behavior and their great potential for use as holographic storage media have been investigated. The physical mechanism explaining these two compartments has the same origin: a low value of the electron diffusion coefficient  $D_e$ .

This Letter describes an extensive investigation of the dynamics inside these blends. Variations of molecular motions inside such structures are related to the physical state. Two techniques are used to probe different processes: photo-correlation spectroscopy (PCS) and forced Rayleigh scattering (FRS).

## 2. Experimental

### 2.1. Sample preparation

The two families of nanocomposites are multicomponent systems where photosensitive molecules are entrapped in a network. The sensitive molecules are Keggin heteropolymetalates (POM), silicotungstate,  $\text{SiW}_{12}\text{O}_{40}^{4-}$ , and phosphotungstate  $\text{PW}_{12}\text{O}_{40}^{3-}$ . They have a spherical shape ( $\approx 10 \text{ \AA}$  diameter) and well-documented redox properties [10]. The structural skeleton is based on an organic–inorganic network.

Type I gel demonstrates that a mixture of tetraethoxysilane (TEOS) and tetraethyleneglycol (TEG) could be used to dissolve high ratios of POM and leads to transparent material.

Type II material shows that organosilanes could be used as the framework of nanocomposites.

An idealized structure of such materials is presented in Fig. 1.

Two different POM concentrations are studied corresponding to 0.2 and 0.6 W/Si<sub>alkoxide</sub>. The following notations will be used: [type]<sub>x</sub> where 'type'

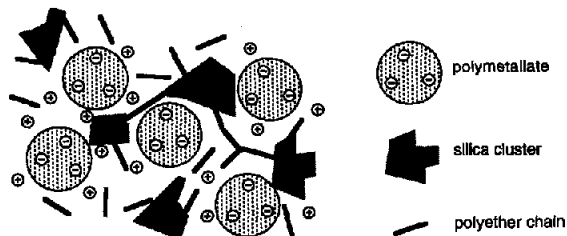


Fig. 1. Schematic of the POM based organic–inorganic nanocomposites.

symbolizes the nature of the matrix (I or II) and the nature of the POM species (P or Si) and  $x$  the [W]/[alkoxide] ratio e.g. [IISi]<sub>0.6</sub> means a system of type II, containing  $\text{SiW}_{12}\text{O}_{40}^{4-}$  ([W]/[alkoxide]=0.6). For reference solutions (dissolution of POM in TEG), it is [TX]<sub>x</sub>.

The synthesis of two representative materials will be described. The gel point,  $t_g$  is defined by the absence of a solution's flow.

[IP]<sub>0.6</sub>. 2.08 g of TEOS ( $10^{-2}$  mol) are added to 1.94 g of TEG ( $10^{-2}$  mol) and 0.45 g of water ( $2.5 \times 10^{-2}$  mol), 1.98 g of  $\text{H}_3\text{PW}_{12}\text{P}_{40}$  ( $5 \times 10^{-4}$  mol) are added, and the blend is vigorously stirred at 60°C. The liquid is poured in the experiment cells.  $t_g$  is six days for [IP]<sub>0.6</sub>.

[IIP]<sub>0.6</sub>. 2.36 g of 3-(2,3 epoxypropoxy)propyl-trimethoxysilane (GPTS) ( $10^{-2}$  mol) and 0.9 g of water ( $5 \times 10^{-2}$  mol) are vigorously stirred and 1.98 g of  $\text{H}_3\text{PW}_{12}\text{O}_{40}$  are added,  $t_g$  is 4 h for [IISi]<sub>0.6</sub>, 22 h for [IIP]<sub>0.2</sub>, and 10 h for [IISi]<sub>0.2</sub>.

### 2.2. Photo-correlation spectroscopy

The light scattering experiments were performed with a helium–neon laser (632.8 nm, 50 mW) and an ALV5000 correlator at  $20 \pm 0.1^\circ\text{C}$ . The translational diffusion coefficient  $D_c$  could be determined ( $D_c/q^2=1$ ). A broad range of time scales is obtained with the multiple Tau technique, and the CONTIN method [11] is used to get the different correlation modes.

Fig. 2 shows typical plots of the autocorrelation functions. The following observations can be made:

- At least, two relaxation modes are present in the different states of the mixtures.
- The slower relaxation mode shifts to longer values with evolution of the process.
- The intensity of the autocorrelation function strongly decreases around the gelation point as a consequence of the variation of the slower mode.

A single correlation time should be obtained in the viscoelastic continuum medium [12]. However, the presence of many relaxation modes has still been observed in hydrogels, polyelectrolytes [13] or for particles entrapped in gels [14]. The first relaxation mode is characteristic of cooperative diffusion of the network, while the second relaxation time has been interpreted as some spatially restricted movements

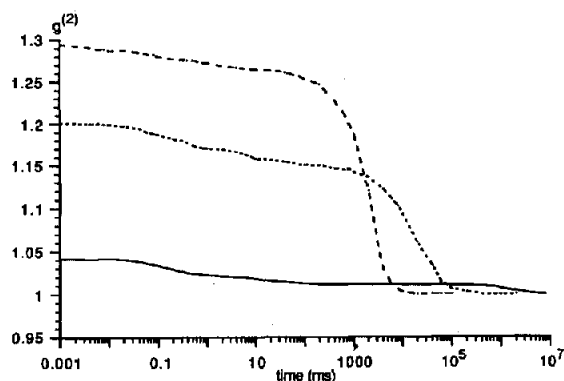


Fig. 2. Typical plots of the time autocorrelation function ( $[\text{HSi}]_{0.2}$ , scattering angle  $45^\circ$ , temperature  $20^\circ\text{C}$ ): (---) After mixing ( $t/t_g=0$ ); (-.-) before gelation ( $t/t_g=0.8$ ); (—) after gelation ( $t/t_g=1.2$ ).

inside the framework. The multiphasic structure of materials I and II could explain such relaxation modes.

### 2.3. Forced Rayleigh scattering

FRS has previously been used to measure the translational self-diffusion coefficient of photosensitive molecules in porous glass [15]. In our materials, the photochromic POM molecules could probe the properties of the materials. The experimental apparatus for production of interference fringes via two-wave mixing has been described previously [9]. Interference patterns were created with a laser tuned to 351 nm ( $2 \times 30$  mW) and checked to produce a grating with 10 nm periodicity. The writing time is monitored to 0.05 s. Reading of the pattern was done in the transmission mode, for the first Bragg angle generated at the wavelength of a He-Ne laser. From the experimental decay, the diffusion coefficient of colored species  $D_e$  was determined [16].

## 3. Results and discussion

### 3.1. Analysis of viscous medium

The results of PCS, FRS and viscosity measurements in TEG/POM solutions are summarized in Table 1. Attention should be paid to the following points:

Table 1

Data obtained for the reference sample (POM/TEG)

Composition	PCS $D_{c1}$ ( $\text{cm}^2 \text{s}^{-1}$ )	FRS $D_e$ ( $\text{cm}^2 \text{s}^{-1}$ )	$\eta$ (mPA s)
[TP] $_{0.2}$	$14 \times 10^{-11}$ <sup>a</sup>	$4.4 \times 10^{-8}$	150
[TSi] $_{0.2}$	$8 \times 10^{-11}$ <sup>a</sup>	$5.8 \times 10^{-8}$	140
[TP] $_{0.4}$	$3 \times 10^{-11}$	$3.5 \times 10^{-8}$	330
[TSi] $_{0.4}$	$6 \times 10^{-11}$	$4.4 \times 10^{-8}$	240
[TP] $_{0.8}$	$3 \times 10^{-11}$	$8.0 \times 10^{-9}$	1370
[TSi] $_{0.8}$	$4 \times 10^{-11}$	$5.8 \times 10^{-9}$	720

<sup>a</sup> A quicker process is measured,  $D_{c2} = (3-5) \times 10^{-8} \text{ cm}^2 \text{ s}^{-1}$ . Viscosity: cone-plate device, shear rate of  $200 \text{ ws}^{-1}$ .

– The decreasing of the value of  $D_{c1}$  and  $D_e$  and an increase of  $\eta$  with the increase of POM ratio.

– A big discrepancy is observed between the diffusion coefficient measured by PCS ( $D_{c1}$ ) and FRS ( $D_e$ ).

– A second relaxation mode is measured for the samples with the lowest POM concentrations.

The corresponding relaxation time  $D_{c2}$  is quite similar to the value of  $D_e$ . The phenomenon measured by the two techniques are different. PCS measures the motion of particles or local inhomogeneities. FRS measures the diffusion of the colored species inside the medium. The main contribution to  $D_e$  is the POM diffusion, while a contribution from the electron hopping mechanism could not be excluded [17].

The PCS measurement slows a slow mode,  $D_{c1}$ , two orders of magnitude lower than the POM clusters themselves. They should correspond to the formation of larger aggregates obtained by clustering of POM or POM-TEG complexes.

### 3.2. Gelation analysis

#### 3.2.1. Type I system

Fig. 3 presents the results of FRS and PCS. The diffusion coefficient of POM (FRS), slowly decreases from  $2 \times 10^{-8} \text{ cm}^2 \text{ s}^{-1}$  at the mixing instant of  $10^{-9} \text{ cm}^2 \text{ s}^{-1}$  at  $2t_g$ . No transition is observed around the gel time, meaning that POM motion does not experience the macroscopic changes. The features measured with PCS are quite different. Just after mixing the reactants, two characteristic modes are measured, around  $4 \times 10^{-10} \text{ cm}^2 \text{ s}^{-1}$  ( $D_{c1}$ ) and  $10^{-6} \text{ cm}^2 \text{ s}^{-1}$  ( $D_{c2}$ ). The values of these two modes are regularly decreasing. This behavior corresponds to a continuous slowing down of the motional correlation

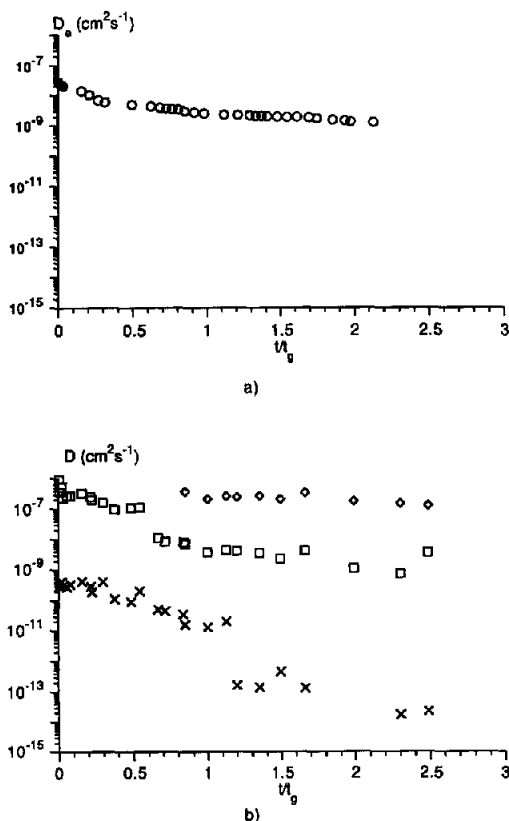


Fig. 3. Type I materials, gelation of [IP]<sub>0.6</sub>. (a) FRS, (○)  $D_e$ . (b) PCS, (×)  $D_{e1}$ ; (□)  $D_{e2}$ ; (◇)  $D_{e3}$ .

time of the clusters reflecting more and more restricted motions. Such a result parallels the strong mass loss of 25% measured during the same delay, and the increase of viscosity. Around  $t/t_g=0.5$ , a splitting of the mode  $D_{e2}$  is measured. Thereafter, the three diffusion coefficients slowly decrease. An abrupt transition of the slower mode occurs around  $t/t_g=1.2$ . Thus, identification of this mode with the cooperative diffusion of the biggest clusters is obvious. The percolation theory explains such a drop from sol to gel, with the spanning of the recipient with the biggest objects [18]. The close values of  $D_{e2}$  and  $D_e$  suggest they should correspond to the self-diffusion of POM entities.  $D_{e3}$  should correspond to the motion of lightweight molecules fragments.

The changes of dynamics observed with the evolution are strongly related to the process leading to gelation. In the reaction with water, TEOS hydrolyzes and condensates to form bushy silica, mostly in the

first couple of hours [14], then releasing ethanol molecules in a few days (30% of the initial mass). Thereafter, most of the chemical reaction steps are finished, and the gelation seems mainly to be the critical time for exhaustion of ethanol molecules. Anyway, one cannot exclude the formation of a few chemical or hydrogen bonds during the same delay.

### 3.2.2. Type II system

Fig. 4 presents the results of FRS and PCS. The FRS of the different systems presents a slow decay of  $D_e$  of one decade from mixing up to gelation. After gelation, a strong decrease of  $D_e$  could be observed in discontinuous stages. They are correlated to the formation of cracks at the surface of the material and an increase of the ethanol evaporation rate. Actually, the

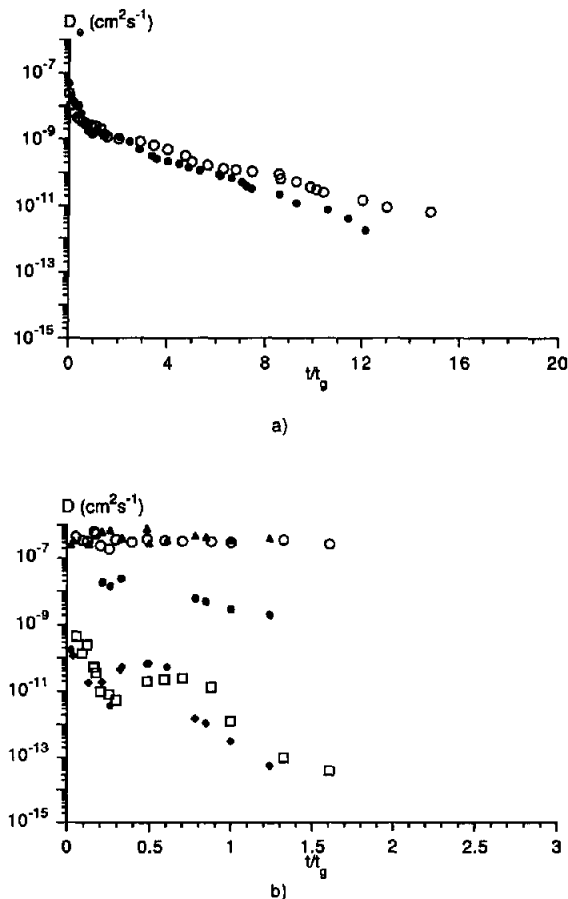


Fig. 4. Type II materials. (a) FRS, (●)  $D_e$  [IISi]<sub>0.2</sub>; (○)  $D_e$  [IISi]<sub>0.6</sub>. (b) PCS, (○)  $D_{e2}$  [IISi]<sub>0.6</sub>; (□)  $D_{e1}$  [IISi]<sub>0.6</sub>; (▲)  $D_{e2}$  [IISi]<sub>0.2</sub>; (◆)  $D_{e3}$  [IISi]<sub>0.2</sub>; (●)  $D_{e1}$  [IISi]<sub>0.2</sub>.

mass loss curves point out that only 2% to 15% of the methanol is removed at the gel point, in regard to the theoretical values of 25%. The remainder of the solvent is removed after gelation through the free surface.

The PCS measurements of  $[\text{IISi}]_{0.2}$  and  $[\text{IISi}]_{0.6}$  present some strong similarities. Like the type I system, two or three relaxation modes are measured and only the slower presents strong variations. Its evolution occurs in three steps: a fall at first ( $0 < t/t_g < 0.2$ ), a kind of plateau, and a second drop of 3 decades ( $0.7 < t/t_g < 1.2$ ). The shape of these curves seems quite independent of the POM ratio.

For the type II system, the gelation kinetics is fast in regard to the evaporation of methanol, which is the by-product of the hydrolysis–condensation reaction of alkoxides. Then, at the gelation point a huge amount of light solvent molecules are entrapped inside the pores, and lead to a high self-diffusion coefficient of POM. After the gel point, the methanol evaporation extends, leading to a gradual decrease of the POM mobility. Mechanical strains appear in the material, and cracks are formed to compensate. They lead to an increase of the area to volume ratio, and a subsequent rise of the evaporation rate. The completeness of the drying leads to a self-diffusion coefficient  $D_e$  of less than  $10^{-11}/10^{-12} \text{ cm}^2 \text{ s}^{-1}$ .

#### 4. Conclusion

This Letter addresses a detailed study of the physico-chemistry of the sol to gel and gel to xerogel transitions in some photochromic nanocomposites. Two optical methods probe different scales inside the matter. FRS gives evidence for the behavior of the photochromic targets, leading to data on the dynamics of POM clusters and thereafter the microviscosity and microstructure inside such systems. These free probes do not experience the sol–gel transition but the rigidification of the system with the loss of solvent. PCS establishes the formation of the gel framework and macrostructure. Gelation corresponds to the strong decrease of the clusters motion, corresponding to the percolation point.

The gelation processes involved in the two systems reflects some totally different features. In the type I mixture, the kinetics of the chemistry is fast in regard to gelation. The gel could be obtained only when

ethanol was evaporated, and then clusters percolate. In type II brews, the gel formation is rapid, due to the formation of silica clusters and polyether chains. Remaining methanol molecules are trapped inside the structure and the drying of the gel occurs a long time after.

#### Acknowledgement

This work was supported by the Minister for Research and Culture of the State of Saarland. The authors gratefully acknowledge support of this work by Conselho Nacional de Pesquisa (PWO) and Alexander Von Humboldt-Stiftung (PJ). Our thanks are due to B. Schaeffer for the viscosity measurements.

#### References

- [1] H. Schmidt, in: *Chemistry, spectroscopy and applications of sol–gel glasses* (Springer, Berlin, 1992) p. 117.
- [2] C. Sanchez and F. Ribot, eds., *Proceedings of the First European Workshop on Hybrid Organic–Inorganic Materials*, Paris (1993).
- [3] S. Sakka and T. Yoko, in: *Chemistry, spectroscopy and applications of sol–gel glasses* (Springer, Berlin, 1992) p. 89.
- [4] R. Winter, D.W. Hua, X. Song, W. Mantulin and J. Jonas, *J. Phys. Chem.* 94 (1990) 2706.
- [5] P. Audebert, P. Griesmar, P. Hapiot and C. Sanchez, *J. Mater. Chem.* 2 (1992) 1293.
- [6] S.D. Hanna, B. Dunn and J.I. Zink, *Mater. Res. Soc. Symp. Proc.* 271 (1992) 651.
- [7] P. Griesmar, C. Sanchez, G. Puccetti, I. Ledoux and J. Zyss, *Mol. Engin.* 1 (1991) 205.
- [8] P. Judeinstein and H. Schmidt, *J. Sol–Gel Sci. Technol.*, submitted for publication.
- [9] P.W. Oliveira, P. Judeinstein, H. Krug and H. Schmidt, *Advan. Mater. Opt. Electr.*, submitted for publication.
- [10] M.T. Pope and A. Müller, *Angew. Chem. Intern. Ed. Engl.* 30 (1991) 34.
- [11] S.W. Provencher, *Comput. Phys. Commun.* 27 (1982) 21.
- [12] T. Tanaka, L. Hocker and G.B. Benedek, *J. Chem. Phys.* 53 (1973) 5151.
- [13] S. Forster, M. Schmidt and M. Antonietti, *Polymer* 31 (1990) 781.
- [14] S.J. Candau, J. Bastide and S. Delsanti, *Advan. Polym. Sci.* 44 (1982) 27.
- [15] J.M. Drake and J. Klafter, *Phys. Today* (May 1990) 46.
- [16] M. Lohfink, *Master Thesis*, Mainz (1988).
- [17] N.A. Surridge, J.C. Jernigan, E.F. Dalton, R.P. Buck, M. Watanabe, H. Zhang, M. Pinkerton, T.T. Wooster, M.L. Longmuire, J.S. Facci and R.W. Murray, *Faraday Discussions Chem. Soc.* 88 (1989) 1.
- [18] F. Family and D.P. Landau, eds., *Kinetics of aggregation and gelation* (North-Holland, Amsterdam, 1984).